

# Surface characterization of a heavy mineral sand with micro-Raman spectrometry

S. POTGIETER-VERMAAK

*Molecular Science Institute, School of Chemistry, University of the Witwatersrand, South Africa*

The main mineral components of the so-called heavy sands (or black sand) are the titanium, zirconium and iron-bearing minerals, rutile, zircon and ilmenite, accompanied by various minor and trace amounts of silicates or phosphates, often present together with the rare earth elements. The investigated samples originated from Richards Bay Minerals (RBM) in South Africa, which is jointly owned by BHP Billiton and Rio Tinto, the largest titanium slag producer in the world. The present study focused on the characteristics of samples originating from various points in the separation plant. The heavy-mineral fractions and concentrates of a representative suite of samples were investigated using various analytical techniques to establish the differences in morphological and elemental compositions at the different points in the plant. These techniques included: reflected light microscopy, micro-Raman spectrometry (MRS), scanning electron microscopy coupled with energy dispersive X-ray analysis (SEM/EDX) and structural and chemical analyser (SCA). All samples comprised a heterogeneous population of zircon and rutile grains with diverse physico-chemical properties, expressed by large differences in colour and trace element chemistry of single grains. The elemental composition proved the presence of the rare earth elements that appeared to coexist with both Ti and Zr minerals. The percentage of grains hosting inclusions, such as anatase, monazite, quartz, spessartine, augite, epidote and actinolite, varied for each sample and could be uniquely characterized by Raman investigations.

Keywords: heavy mineral sands, micro-Raman spectrometry, elemental analysis

## Introduction

Heavy minerals are detrital grains of minerals with high density ( $>2.7 \text{ g cm}^{-3}$ ) that occur as accessory minerals in quartz sands. These grains are derived from the eroding source rocks and may be distinctive of particular types of rock. Heavy mineral sands (HMS) include ore minerals that may be concentrated sufficiently to form economic deposits—called placer deposits. Placer deposits can form in alluvial channels, on beaches, or on marine abrasion surfaces. Identification is based on their physical properties. Primary separation from the majority of quartz grains involves a gravitational separation process, followed by a magnetic separation based on their differences in magnetic properties (Snyders, 2007).

South Africa is among the global players in the economically exploitable placer deposit mining and is the second largest producer in the world, after Australia, contributing about 23%–30% of the global production of minerals concentrated from HMS (TZ Minerals, 2001). Of this, 90% accounts for ilmenite production, with rutile the remaining 10% (<http://www.ticor-sa.com/>). South Africa and Australia contain the largest commercial zircon deposits, and, according to the United States Geological Survey (2001), have the largest zircon reserves. Ilmenite, zircon and rutile are the main minerals produced from the extensive beach placer deposits located along the eastern, southern and north-eastern coasts of South Africa. Smaller deposits are located on the west coast of South Africa, north of Cape Town. The deposits are mainly mined for rutile ( $\text{TiO}_2$ ), ilmenite ( $\text{FeTiO}_3$ ) and zircon ( $\text{ZrSiO}_4$ ). Ilmenite and rutile are accompanied by garnet, pyroxene, hornblende,

feldspar, tourmaline, epidote, kyanite and staurolite. The source of the ilmenite is believed to be Drakensberg volcanics and post-Karoo dolerites, whereas the rutile and zircon have been eroded from granites and gneisses. Rutile is present as a major mineral and the ilmenite, leucoxene and zircon as minor minerals. Trace minerals include haematite, anatase, monazite, magnetite, chromite, pyrite, sphene and goethite.

The mineral beneficiation process involves flotation, magnetic and electrostatic separation methods (Snyders, 2007). Successful beneficiation therefore strongly depends on the differences in their physical and chemical properties, which is intrinsic to the surface chemistry. Previously these minerals have been chemically characterized by means of X-ray fluorescence spectrometry (XRFS), X-ray diffraction (XRD), stereomicroscopy, optical microscopy and scanning electron microscopy (SEM) (Reynecke and v.d. Westhuizen, 2001). Although Raman spectrometry is commonly used in the fingerprinting of minerals due to their strong characteristic inelastic scattering, and therefore provides valuable information on the intrinsic mineralogical features (Hopep *et al.*, 2001), papers on Raman characterization of HMS samples are very limited. Raman spectrometry has a distinct advantage over the other techniques in that it could also be utilized in in-stream process control monitoring (<http://www.minerals.csiro.au/main/pg2.asp?id=36873>), especially in conjunction with SEM/EDX, which will provide elemental concentrations in addition to the mineral fingerprint obtained by the Raman spectrometer (Godoi *et al.*, 2006).

The aim of the present study was to focus on the surface characteristics of samples originating from various points in a separation/concentration plant. The heavy-mineral fractions and concentrates of a representative suite of samples were investigated using mainly transmitted/reflected light microscopy and micro-Raman spectrometry as analytical techniques. One sample was also investigated with a structural chemical analyser, which is in essence a combination technique, analysing the same spot sequentially with Raman and SEM/EDX. All samples studied comprised a heterogeneous population of zircon and rutile grains with diverse physico-chemical properties. This was expressed by large differences in colour and trace element chemistry of single grains. The percentage of grains hosting inclusions, such as anatase, monazite, quartz, spessartine, augite, epidote and actinolite, varied for each sample and can be uniquely characterized by Raman investigations.

The fast, non-destructive nature of Raman analyses makes it ideal for sample characterization and subsequent adaptations to the production process and conditions to ensure continued optimum recovery of the valuable minerals. This is an aspect of process sample analysis that has been ill-exploited to date and offers substantial scope and potential for utilization in process optimization and troubleshooting procedures.

## Experimental

### Materials

Samples of the non-magnetic fraction of an HMC concentration plant were analysed. The samples originated specifically from the non-conducting fraction (zircon rich) and were taken at various stages in its clean-up process. The samples were investigated in terms of their molecular characteristics, with special attention to their surface properties using micro-Raman spectrometry (MRS). Furthermore, one sample was also analysed for its elemental composition using SEM-SCA. Samples were prepared by contacting carbon tape with some of the concentrate and brushing off the excess to facilitate well-separated particles for easy analysis.

### Analytical techniques

- *Optical microscopy* (Olympus SZX12) was performed on all the samples, using various magnifications, to characterize the particles.
- *Micro-Raman spectrometry* (Renishaw InVIA confocal scanning spectrometer, fitted with 514 and 785 nm excitation sources) on numerous particles of each sample provided information about the chemical composition and identity of the sample. The instrument was equipped with a Peltier cooled charged coupled device detector and a spectral width slit corresponding to a resolution of  $1\text{ cm}^{-1}$ . Normal working distance objectives, with 20X, 50X and 100X magnifications and numerical apertures of 0.40, 0.75 and 0.90, resulting in a lateral spatial resolution of 1–5  $\mu\text{m}$ , were used. The number of acquisitions varied between 1 and 16 and the acquisition time from 10 to 40 s in order to reduce the signal to noise ratio for each particular analysis measured over a spectral range of 3 200 to 100 wavenumbers. The laser power was varied between 1 mW and 10 mW, depending on the compounds of interest detected. Conditions in each case are mentioned in the relevant figure captions. Various spot

analyses on the different particles were performed to ensure that representative results were obtained. Data acquisition was carried out with the Spectracalc software package GRAMS (Galactic Industries, Salem, NH, USA). Spectral identification was performed by comparison with spectra from an in-house library as well as a commercially available spectral library (Renishaw Minerals Spectral Library operated with GRAMS software).

- *MRS-SEM-EDS* (Renishaw SEM-SCA) on several particles of one sample provided chemical, structural and elemental information. The instrument is equipped with a Renishaw InVIA confocal spectrometer and a JEOL JSM 6300 SEM/EDS. A Si(Li) X-ray detector coupled to a PGT (Princeton Gamma Tech, Princeton, NJ, USA) system was employed for acquiring the X-ray spectra (acquisition time was 20 s). The typical energy of electron bombarding was 30 keV and a beam current of 1 nA was used.

## Results and discussion

### Raman investigation

In general the samples investigated comprised a heterogeneous population of minerals, often present in different polymorphs, and were dominated by zircon ( $\text{ZrSiO}_4$ ) and the rutile polymorph of  $\text{TiO}_2$ . The mineralogical phases were easily identified by Raman spectrometry. The diverse physico-chemical properties of the individual grains were expressed by the various shapes, colours and trace elemental composition, as determined by optical and scanning electron microscopy complemented with EDS. The excellent suitability of Raman analysis, which is performed on the sample without any sample preparation or alteration of the surfaces, is illustrated in the following figures and discussion, where attention is paid to each sample in more detail.

### Sample 1

The sample was taken from the Zr-rich stream and the various minerals identified are illustrated in Figures 1–4. This sample was dark brown in colour due to the carbon coating it received to improve conductivity during the concentration and separation process. Grey, large and smooth- or sharp-edged oval-shaped particles were ubiquitous and were identified as zircon. The brown colour of the sample was attributed to the various shades of yellow, reddish, orange and pink particles present. The black stones were very shiny, in the minority and identified to be mainly rutile, although a small number of yellow and red rutile stones were also identified and the presence of titanite ( $\text{CaTiSiO}_5$ ) was also demonstrated. The other yellow-to-orange grains were identified as brookite ( $\text{TiO}_2$ ), monazite ( $\text{La,Ce,NdPO}_4$ ) and various silicates such as sphene  $\text{CaTi}(\text{SiO}_4)(\text{O,OH,F})$ . A very small number of particles were dark-grey and proved to be augite ( $(\text{Ca,Na})(\text{Mg,Fe,Al})(\text{Si,Al})_2\text{O}_6$ ) and the greenish epidote  $\text{Ca}_2(\text{Al,Fe})\text{Al}_2\text{O}(\text{SiO}_4)(\text{Si}_2\text{O}_7)(\text{OH})$  also appeared.

### Sample 2

This sample can best be described as a brown sand with a large number of grey particles and discretely placed black particles. The mineralogical make-up of this sample was similar to that of sample 1 and the lighter colour could be ascribed to the fact that it was not coated with carbon yet.

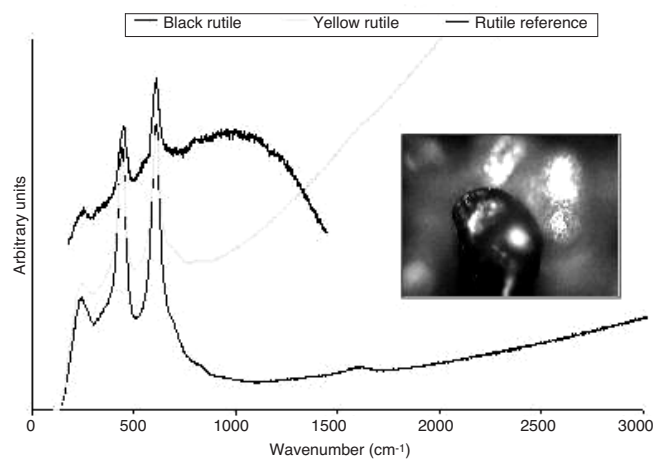


**Figure 1. Raman spectra of yellow and black rutile, accompanied by the digital light image**

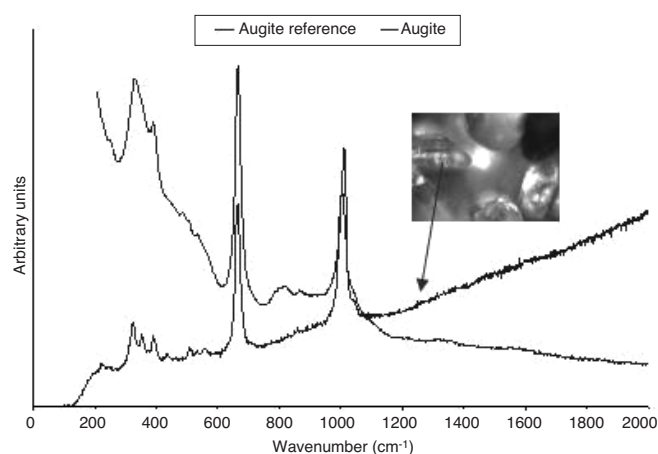


**Figure 4a. Raman spectrum of augite**

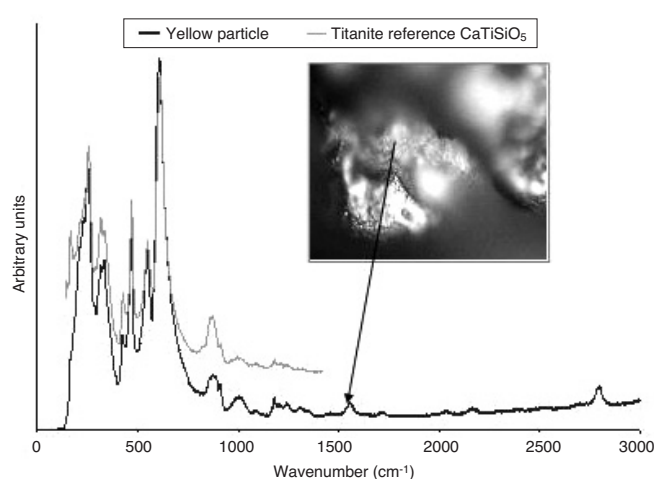


**Figure 2. Raman spectra of yellow titanite inclusion on a black rutile particle, accompanied by the digital light image**

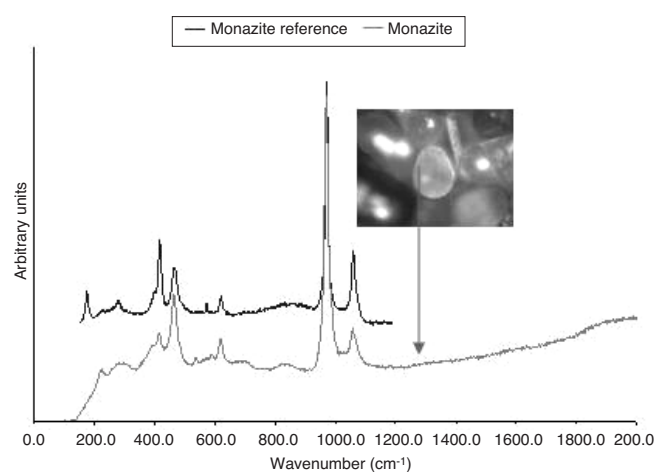


**Figure 4b. Raman spectrum of monazite**

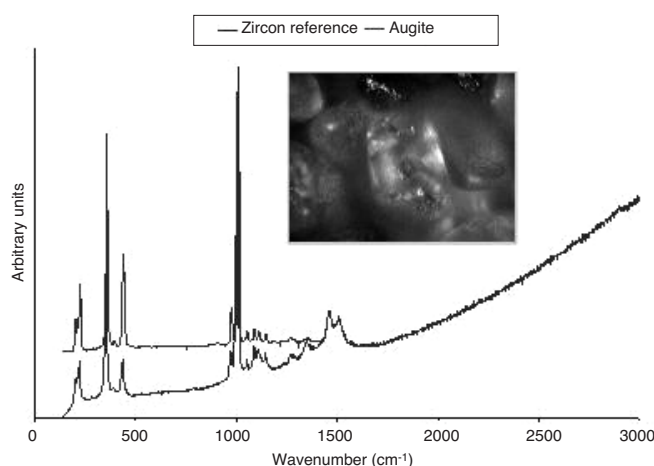


**Figure 3. Raman spectra of zircon particles with a red covering, accompanied by the digital light image**

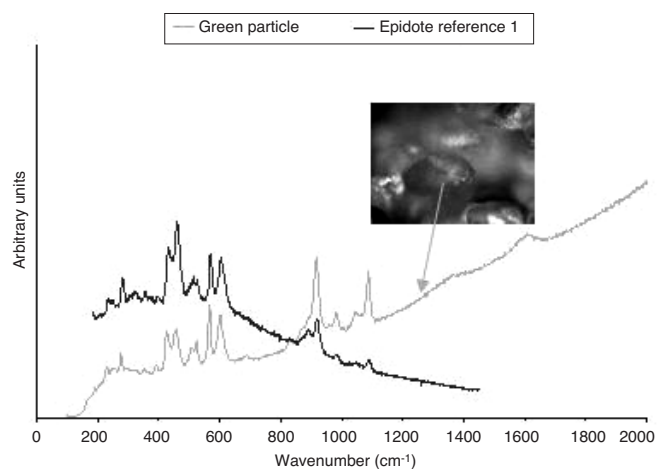


**Figure 4c. Raman spectra of epidote**

### Sample 3

This sample originated downstream from samples 1 and 2 and was the Zr concentrate. This was indeed confirmed during the analysis and the main body of the sample comprised grey zircon particles. Some silicate minerals

were also identified as before, such as actinolite ( $\text{Ca}_2(\text{Fe,Mg})_5\text{Si}_8\text{O}_{22}(\text{OH})_2$ ), as illustrated in Figure 5, and a limited number of Ti-rich particles were observed.

### Sample 4

This sample originated from the conductive part of sample 1 and was supposed to be free of Zr-rich particles and be

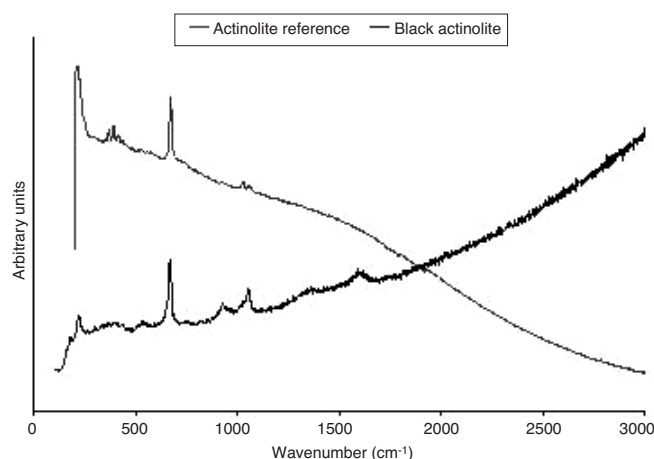


Figure 5. Raman spectrum of actinolite

mainly Ti-rich in character. It was, however, found that this sample still contained a substantial number of Zr-rich particles apart from the larger Ti-rich component. It was a fairly dark sand and appeared almost black. Most of these black stones were rutile and usually in an egg-shape. Occasionally dark grains of augite also appeared. The grey stones were in the minority and usually of irregular shape and sometimes had a colourful yellow shine. They are cuboid shaped, often with sharp edges. The grey mineral was again identified as  $\text{ZrSiO}_4$ . Zircon grains sometimes were covered with a reddish or orange substance. The coloured stones proved to be either anatase, anatase+rutile, pure rutile, brookite, sphene or spessartine ( $\text{Mn}_3\text{Al}_2$

( $\text{SiO}_4$ )<sub>3</sub>), some of whose Raman spectra and digital light images are shown in Figure 6.

From Figure 6 one can see that the different polymorphs of titania can occur intergrown in one particle, as evidenced by the Raman spectrum portraying both rutile and anatase character. This sample was covered in places with a red substance that appeared amorphous, potentially indicating secondary alteration, and proved to be anatase in some instances. Sometimes this substance fluoresced to such an extent that it could not be identified.

### SEM-SCA investigation

The Ti-rich sample was also analysed by the SEM-SCA. It is evident from the elemental X-ray mapping, illustrated in Figure 7, that the separation process was indeed not 100% successful due to the presence of several Zr-containing particles.

It was also ascertained that the Ti particles were strongly associated with O and the Zr particles with O and Si, as illustrated in Figure 8.

Some of the Zr-bearing grains seem to be heterogeneous, partly associated with Si and O. The corresponding Raman spectra illustrated the different polymorphic forms of titania and classified the Zr-Si-O association as zircon ( $\text{ZrSiO}_4$ ). The two polymorphs of titania encountered are illustrated in Figure 9.

It is interesting to notice the coexistence of Al with the anatase and its absence from the rutile.

### Conclusions

MRS gives a fast and appropriate method of analysing of HMCs for all the various minerals and their different

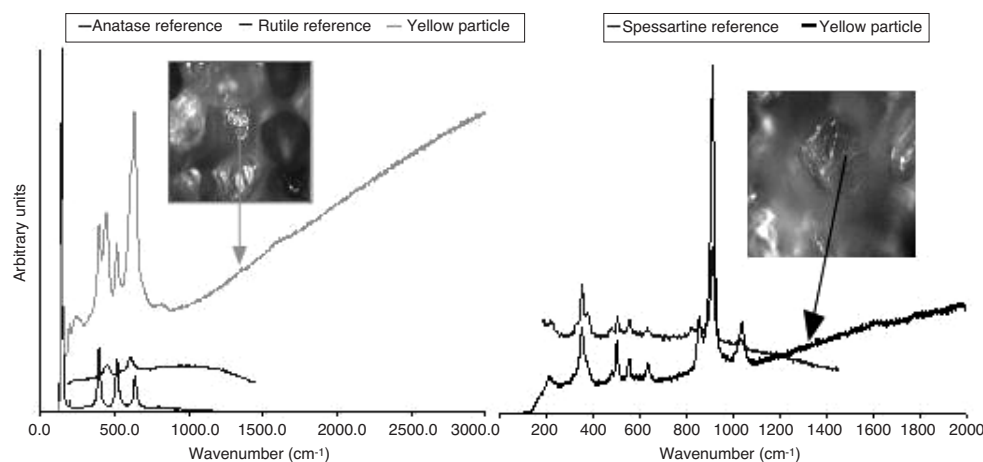


Figure 6. Raman spectra of anatase mixed with rutile and spessartine, accompanied with the digital light images

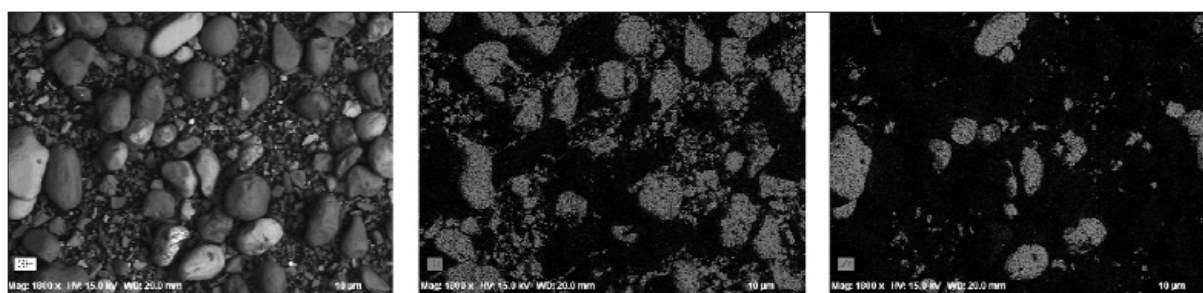


Figure 7. LV-SEM image, Ti X-ray map and Zr X-ray map



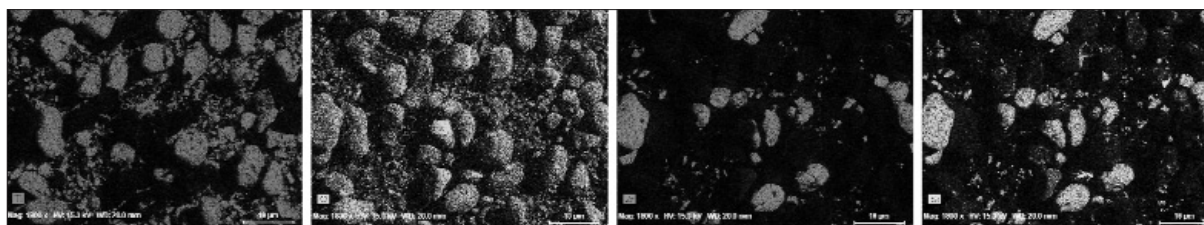


Figure 8. Illustrating the Ti, O, Zr and Si associations

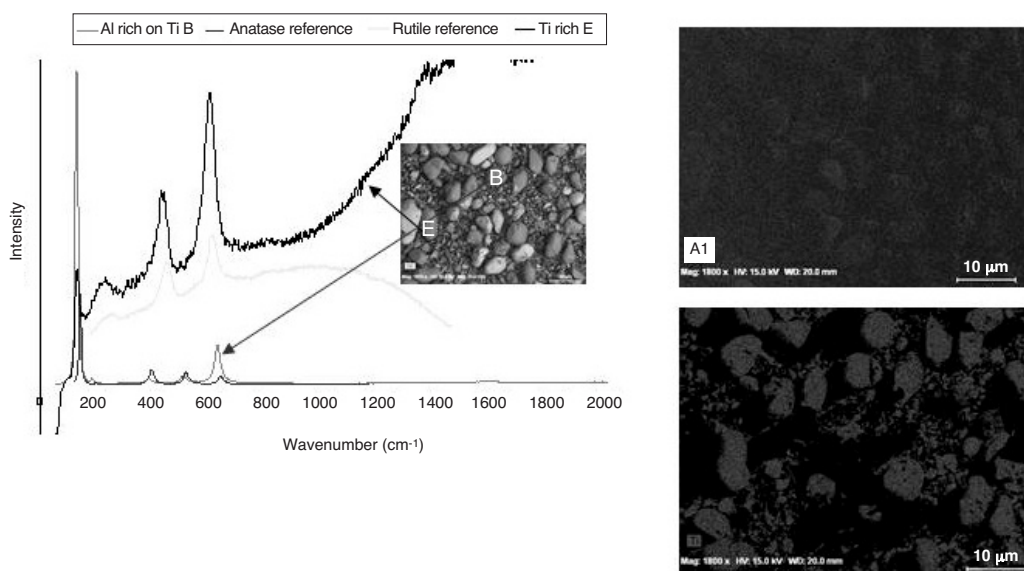


Figure 9. Corresponding Raman spectra of the titania polymorphs found in the sample

polymorphs. Raman spectrometry has proven to be suitable for in-stream or on-line analysis of minerals (<http://www.minerals.csiro.au/main/pg2.asp?id=36873>) and the data obtained in this investigation illustrates the benefit of it for the HMC industry and could successfully be utilized to do a fast *in situ* estimation of the efficiency of the separation process.

The results clearly illustrated that the different titania polymorphs are associated with different other elements and phases in the mineral samples, e.g. anatase seems to occur together with Al. The unique fingerprinting ability illustrated by the analysis of samples with the SEM-SCA illustrated that the combination of MRS and EDS could be utilized for fast troubleshooting and problem solving in the plant process, when separation efficiency is not optimum. Therefore, by coupling existing routine X-ray fluorescence analysis with on-line Raman spectrometry, fast non-destructive in-stream process control monitoring could be facilitated.

### Acknowledgements

Renishaw is thanked for their technical assistance and use of equipment. Richards Bay Minerals are acknowledged for providing the samples for analysis.

### References

1. GODOI, R.H.M., POTGIETER-VERMAAK, S.S., DE HOOG, J., KAEGI, R., and VAN GRIEKEN, R.

Substrate selection for optimum qualitative and quantitative evaluation of single atmospheric particles using nano-manipulation, sequential thin-window electron probe X-ray microanalysis and micro Raman Spectrometry, *Spectrochim Acta B*, vol. 61. pp. 375–388 (2006).

2. HOPEP, G.A., WOODSY, R., and MUNCE, C.G. Raman microprobe mineral identification, *Min. Eng.*, 2001, vol. 14, no. 12. pp. 1565–1577.
3. <http://www.minerals.csiro.au/main/home.asp?view=About>; On-line Analysis and Control Program; updated 19/01/2006; accessed 04/02/2006.
4. <http://www.ticor-sa.com/>. 2004. Accessed: 10/05/2005.
5. REYNECKE, L. and VAN DER WESTHUIZEN, W.G. Characterisation of a heavy mineral-bearing sample from India and the relevance of intrinsic mineralogical features to mineral beneficiation, *Min. Eng.*, 2001, vol. 14, no. 12. pp. 1589–1600.
6. SNYDERS, E. The development of Zircon as a superior opacifier, D Tech Thesis, 2007.
7. TZ MINERALS INTERNATIONAL PTY LTD. The Global Zircon Industry—A five year outlook with a special focus on China. 2001.

